

# Microstructure and Dielectric Properties of ZnO-SiO<sub>2</sub>-NiO Composite

Osama A. Desouky<sup>1</sup>, Mostafa M. H. Khalil<sup>2</sup>, Hamdy A. Kattab<sup>2</sup>

<sup>1</sup>Higher Institute of Engineering (BHIE), Bilbis, Sharqia, Egypt

<sup>2,3</sup>Chemistry Department, Faculty of Science, Ain Shams University, 11566 Abbassia, Cairo, Egypt

**Abstract:** *The effect of SiO<sub>2</sub> addition on the properties of ZnO-NiO composite were investigated. The samples with different SiO<sub>2</sub> concentrations were fabricated by the conventional ceramic method and sintered at 1000<sup>o</sup>C. The results of XRD show that Zn<sub>2</sub>SiO<sub>4</sub> and Ni<sub>2</sub>SiO<sub>4</sub> generate during sintering, The relative density for the samples increased as the NiO content increased; also it decreased as the SiO<sub>2</sub> content increased. The presence of 0.1 wt% ZrO<sub>2</sub> remained as chemically stable second phase particles among ZnO grains, and thus retarded densification and inhibited the grain growth of ZnO in the liquid phase sintering. The AC resistivity decreases with increasing frequency at room temperature.*

**Keywords:** ceramics - ZnO- NiO- SiO<sub>2</sub>- composite

## 1. Introduction

The study of composite materials, i.e., mixtures consisting of at least two phases of different chemical compositions, has been of great interest from both fundamental and practical standpoints. The macroscopic physical properties of such materials can be combined so as to produce materials with a desired average response [1]. Composites have good potential for various industrial fields because of their excellent properties such as high hardness, high melting point, low density, low coefficient of thermal expansion, high thermal conductivity, good chemical stability and improved mechanical properties such as higher specific strength, better wear resistance and specific modulus [2,3]. Composites are used in making solar cells, optoelectronic device elements, laser diodes and light emitting diodes (LED), industrial applications in aircraft, military and car industry. Besides this, the composites getting from the transition metal oxides are started to use as humidity and gas sensors [4]. ZnO oxide is a II-VI compound semiconductor with wurtzite structure [5]. ZnO films have been investigated as electronic and optoelectronic device materials such as, transparent conductors, solar cell windows, gas sensors and surface acoustic wave devices because of their n-type conducting with an optical transparency in the visible range. Various ZnO film preparation methods have been used; magnetron sputtering, spray pyrolysis, chemical vapor deposition (CVD), pulsed laser deposition and sol-gel process [6].

Zinc oxide (ZnO) on the other hand is one of the versatile and technologically important semi conducting material because of its typical properties such as transparency in the visible range, high electrochemical stability, direct band gap (3.37)eV, absence of toxicity, abundance in nature etc. [7]. NiO is a transition metal oxide that has several potential applications, such as solar thermal absorber, electrodes for battery and photoelectron-catalysts [6]. Nickel oxide (NiO) thin films are promising materials with excellent electrochromic properties. Other important application of Nickel oxide films includes preparation of alkaline batteries (as cathode material), antiferromagnetic layers and P-type

transparent conducting films [8]. NiO is a p-type semiconductor with a band gap ranging from 3.6 eV to 4.0 eV transparent to ultraviolet (UV), visible and near infrared radiation. Silicon dioxide has been used as primary gate dielectric materials in field-effect device since the advent of first integrated circuit [9]. The other point of interest of silicon dioxide (SiO<sub>2</sub>) compound in the industrial domain is due to its various qualities (electrical, optical, chemical and thermal properties). It is used widely in the optical and electronic applications (opto-electronic devices, optic fibers, etc). The crystal structure of silicon dioxide (SiO<sub>2</sub>) has attracted the attention of many researchers because it is one of the most fundamental oxide systems [10]. It has low interfacial defect density, high melting point, large energy gap, high resistivity and good dielectric strength [11]. Nickel oxide (NiO) and Zinc oxide (ZnO) thin films have been prepared by various techniques, such as thermal evaporator, sputtering, sol-gel, spray pyrolysis, chemical vapour deposition and chemical bath deposition (CBD). For instance, work has been done on the microstructure, electrical and optical properties of ZnO-NiO-SiO<sub>2</sub> nanocomposite synthesized by Sol-Gel Technique [12]. Other work carried out in this area includes synthesis and characterization of ZnO-NiO composite nano particles by solution method etc [13]. Among all these different techniques for deposition, chemical bath deposition was successfully used to obtain ZnO/NiO multilayer thin films due to its relative simplicity, low cost and potential application for large area deposition [14]. In this study, the polycrystal ZnO-NiO-SiO<sub>2</sub> composite material was prepared by solid state method. The physical and electric and of the obtained composite materials were investigated.

## 2. Material and Methods

The powder was prepared using the mixed method in alcoholic medium. All the oxides used were analytical grade: ZnO, NiO, SiO<sub>2</sub> and ZrO<sub>2</sub>. The weight compositions were shown in Table. 1. The starting materials selected were ZnO, NiO, SiO<sub>2</sub> and ZrO<sub>2</sub> in powder form and all the materials were taken in the form of analytical grade. The prepared

ZnO, NiO, SiO<sub>2</sub> and ZrO<sub>2</sub> was wet ground in a ball for a period of 4 hours to pass 200 mesh sieves. The slurry was dried overnight. Batches were abbreviated as S<sub>1</sub>, S<sub>2</sub>, S<sub>3</sub>, S<sub>4</sub>, S<sub>5</sub>, and S<sub>6</sub> wet milled to ensure through mixing of the different compositions then dried at 110 °C. Two discs were used; the first one has 1.2 cm diameter and 0.2 cm thickness. These two discs were processed by a semi-dry press method under 70 KN. Small specimens were subjected to thermal treatment to select the proper maturing temperature for each mix. Three discs were always fired in muffle kiln with a rate of heating of 5 °C /min in the temperature range between (1000 to 1300 °C) and for 2 hours. The sinterability of the different samples was determined in terms of physical properties. These sintered samples were used for morphological, structural and electrical characterizations. The XRD of different mixes were examined by using Philips apparatus type 170, a vanadium (λ=1.54 Å) and Ni-filter in Metallurgy Research Center, Egypt. A continuous plot of intensity for 2θ values 4 to 80 was made at a scanning speed of 1°/ minute, with a paper speed of 10 mm/min. Both surfaces of the samples were lapped and ground with SiC paper and polished with Al<sub>2</sub>O<sub>3</sub> powder to a mirror like surface. The polished samples were thermally etched at 900°C for 30 min. The surface microstructure was examined by a scanning electron microscope (SEM, Joel- JEM. T 200). DTA locates the ranges corresponding to the thermal decomposition of different phases in paste, while TG measures the weight loss due to the decomposition. TG coupled with DTA makes it possible for the hydration reaction to be followed qualitatively, semi-qualitatively and quantitatively. Such thermal analysis is useful to observe the evolution of the hydration and especially to estimate the process of different reaction. Although these techniques are more suitable for studying hydration at later stages, they can be used as here, to consider the early phase of hydration accelerated by high temperature curing. Concerning DTA, 40µm powder specimens were placed in a refractory steel crucible and analyzed using a hybrid system with oven-drying at a heating rate of 5.8 °C/min up to 95 °C. Sample masses ranged from 1.00 to 1.10g. In the case of TG, the specimen (40 µm powder) was introduced into a quartz crucible and analyzed using system at a heating rate of 7.5°C/min up to 600°C. Masses of sample were between 200 and 220mg. No trace of calcium carbonate was detected during analysis as the freeze-drying technique prevented carbonation of the sample hence thermo grams will be presented up to 600 °C for DTA and 650°C for TG . The

PM 6304 program able automatic RCL meter was used for precise measurements of resistance, capacitance and inductance. From the measured values of capacitance, the dielectric constant at all frequency from 50 Hz – 5MHz was calculated at constant temperature . The respective permittivity [ε-] was calculated according to the following

$$\text{relations: } \epsilon' = \frac{Cd}{\epsilon_0 A}, \text{ Where } C = \text{capacitance in Farad.}, d =$$

thickness of specimen in m.,  $\epsilon_0 = 8.85 \times 10^{-12}$  F/m, A = area of specimen in m<sup>2</sup>. Also from the values of resistance R conductivity (σ) was calculated from the following relation:

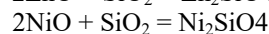
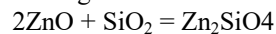
$$\sigma = \frac{d}{RA}, \text{ where } R: \text{resistance, } d = \text{thickness of specimen in m and } A = \text{area of specimen in m}^2.$$

**Table 1:** Composition of Different Mixes in mol%

Oxides/ mixes	ZnO mol%	NiO mole%	SiO <sub>2</sub> mole%	ZrO <sub>2</sub> mole%
S <sub>1</sub>	40	55	5	0.1
S <sub>2</sub>	30	60	10	0.1
S <sub>3</sub>	40	40	20	0.1
S <sub>4</sub>	40	35	25	0.1
S <sub>5</sub>	40	30	30	-
S <sub>6</sub>	30	30	40	0.1

### 3. Results and Discussion

XRD patterns of samples sintered at 1000 °C are shown in Fig. 1. It is easy to identify the main phase ZnO , NiZnO, NiO , zinc silicate and nickel silicate by fitting d spacing data. The results show that Zn<sub>2</sub>SiO<sub>4</sub> and Ni<sub>2</sub>SiO<sub>4</sub> generate during sintering, but the d-spacing data do not exactly match with those of JCPDS card. So a reaction may occur during furnace heating as follows:



Then Zn<sub>2</sub>SiO<sub>4</sub> and Ni<sub>2</sub>SiO<sub>4</sub> crystallized at the ZnO boundary during furnace cooling and formed potential barrier, and there is a little difference in d-spacing between Zn<sub>2</sub>SiO<sub>4</sub> in the samples and JCPDS card. Therefore, the crystallized Zn<sub>2</sub>SiO<sub>4</sub> is a solid solution dissolving and other elements. SiO<sub>2</sub> does not react completely with others at 1000 °C because of the evidence of SiO<sub>2</sub> existing in the sample sintering at 1000 °C showed in the XRD patterns.

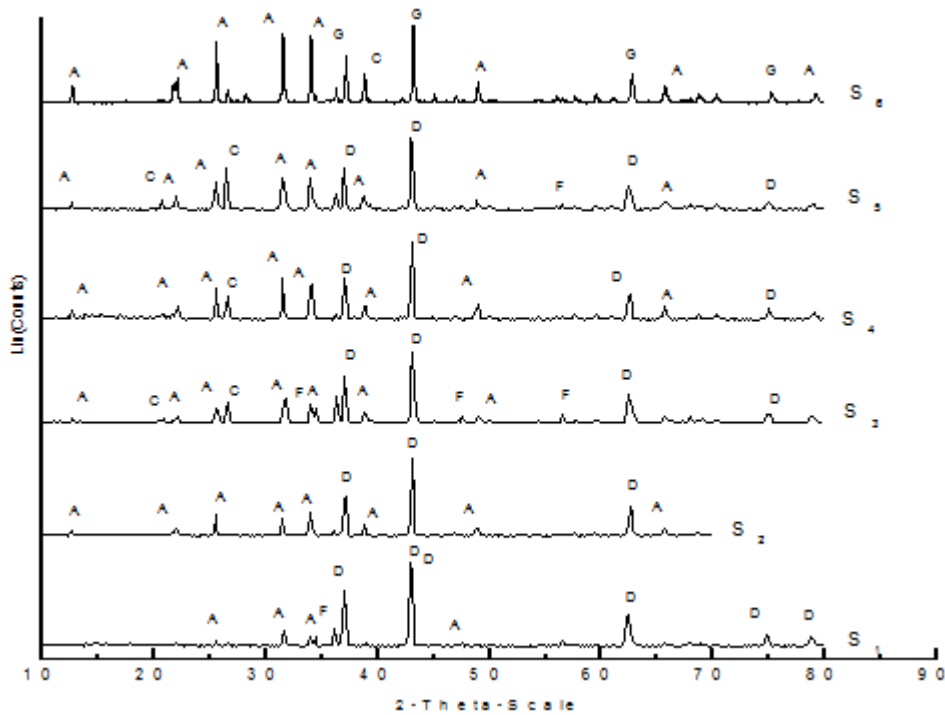


**Figure 1:** XRD patterns of different mixes

Where A: Zinc silicate  $Zn_2(SiO_4)$ , B: Nickel silicate,  $Ni_2(SiO_4)$ ,  
 C: Quartz, D: Nickel Zink Oxide, F: Zink Oxide, G: Nickel Oxide.

The relative density for the fired samples in the temperature range between 1000 and 1300 °C is illustrated in Fig. 2. The relative density equals the theoretical density of a sample divided by its apparent density. The relative density for the samples increased as the NiO content increased; also it decreased as the  $SiO_2$  content increased. Although high densification rate in all samples took place at 1300 °C, it is interesting that only samples  $S_1$  and  $S_2$  have better sintering behavior. At 1300 °C, the relative density of samples  $S_1$  and  $S_2$  have reached 95%, which indicates that samples  $S_1$  and  $S_2$

get to almost full densification. Such a high rate of densification for sample  $S_1$  is thought to be attributed to the lowest glass transition temperature and the viscous glass phase during the firing process [15,16]. The highest densifications are obtained at high sintering temperatures and high sintering times, i.e the bulk density of ZnO-  $SiO_2$  samples with NiO additions increases sharply with increasing temperature and has a constant value above 1000°C .

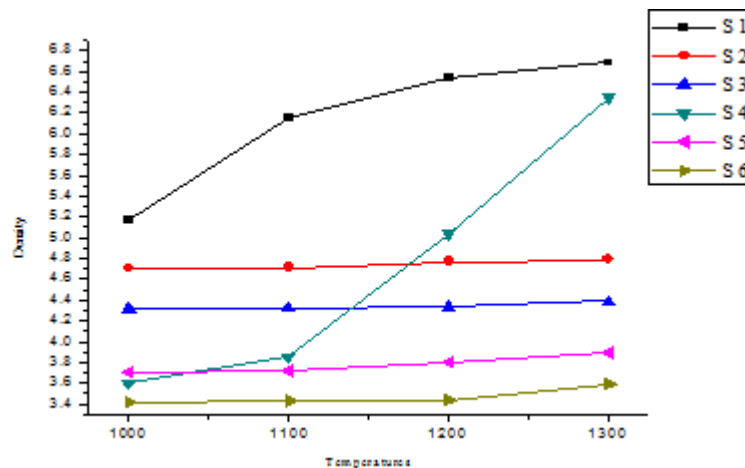


**Figure 2:** Relative density as a function of temperature

Fig. 3. shows the differential thermal analysis DTA thermogram of sample [G(I)S2] which containing 40%wt ZnO, 50%wt NiO, 10%wt  $SiO_2$  and 0.1%wt  $ZrO_2$ . The thermogram shows endothermic effect in which, the onset of the

peak at 32.2°C , the offset at 297.1 °C, the mix / min at 104.1 °C is equal to  $-16.436\mu v$ , and heat change is equal to  $-1220.808 \mu V/s/mg$ .

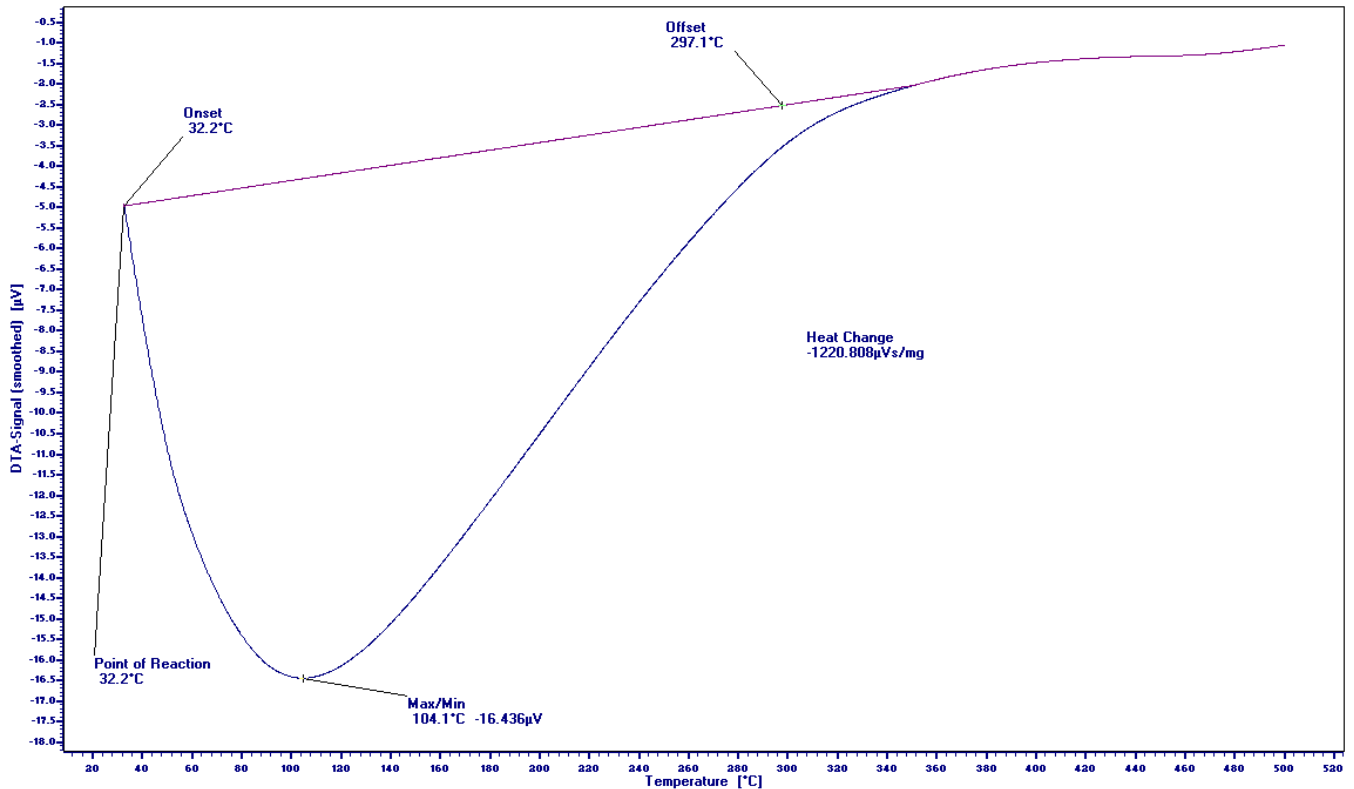


Figure 3: Show the DTA thermogram of sample S2

Fig.4. shows the TG thermo gram of sample S<sub>6</sub> ,in which, mass of the sample at 56.3 °C is equal to 9.056 mg, mass of the sample at 207.5 °C is equal to 8.493 mg, and mass change is equal to -0.56 mg. In addition, mass of the sample at 207.5 °C is equal to 8.493 mg, mass of the sample at

268.9 °C is equal to 7.975 mg, and mass change is equal to -0.52 mg. In addition, mass of the sample at 344.2 °C is equal to 7.758 mg, and mass change is equal to -0.22 mg.

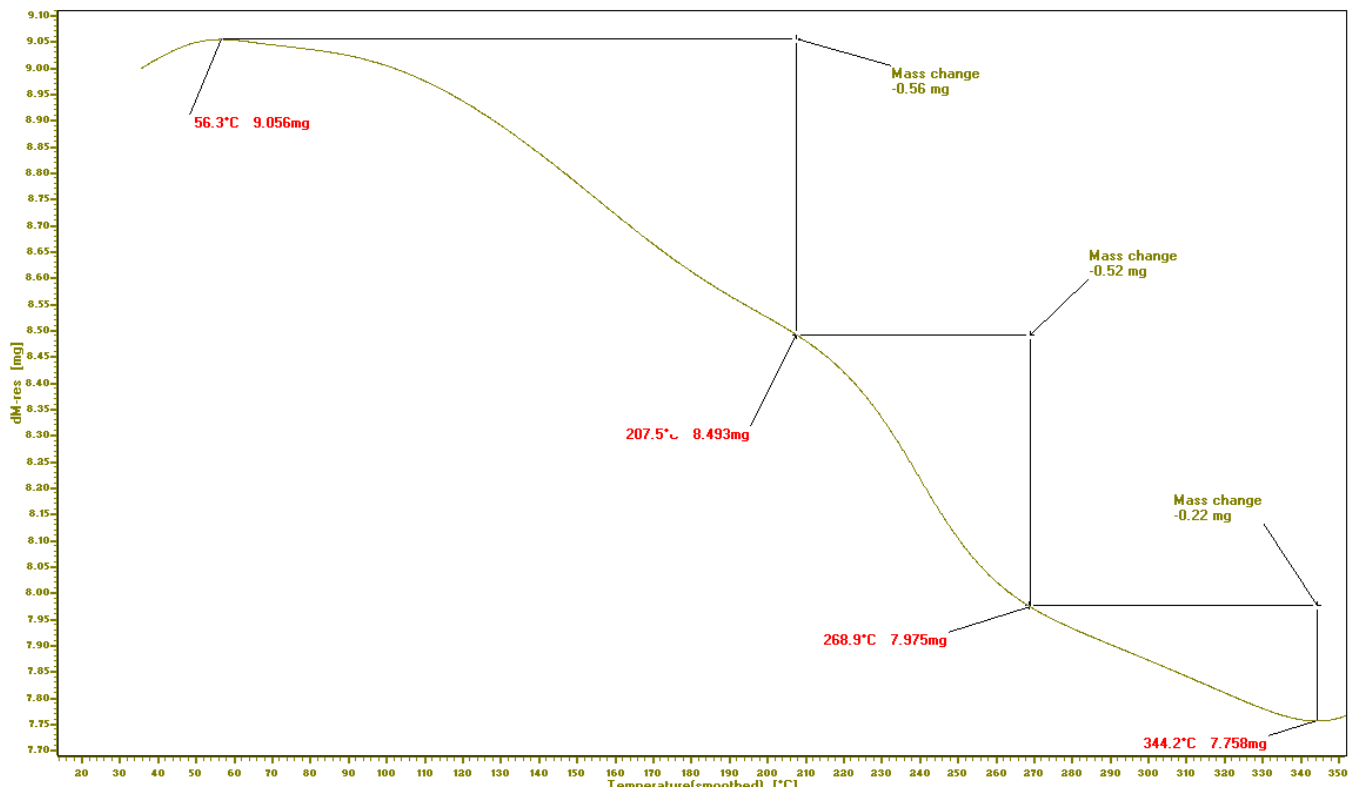


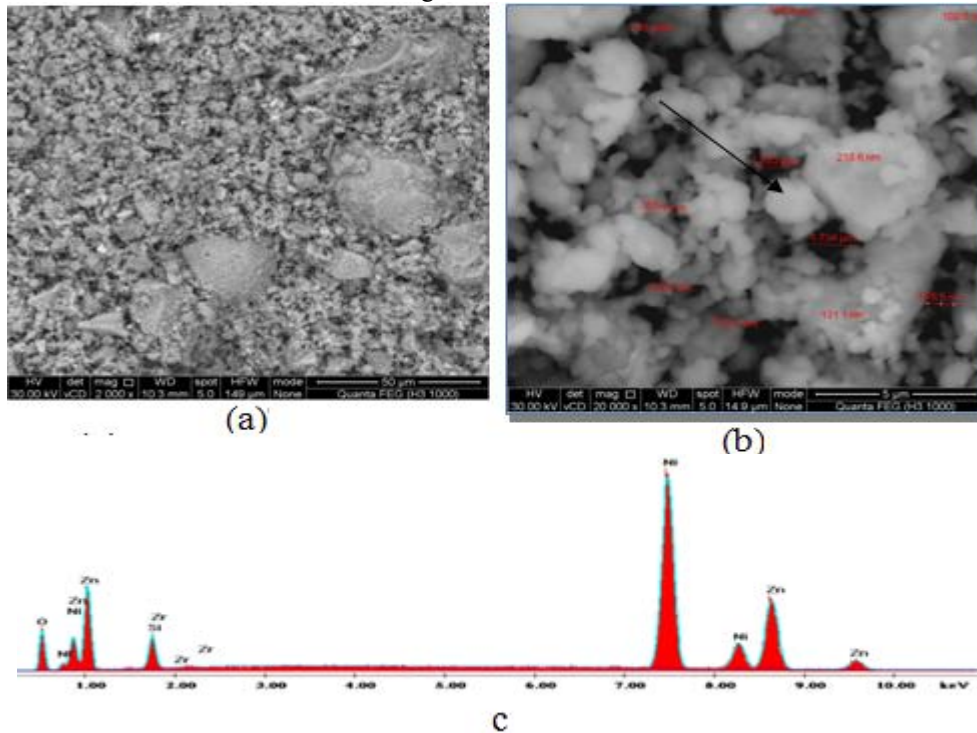
Figure 4: Shows the TG thermo gram of sample S<sub>6</sub>

The microstructure of ZnO-NiO-SiO<sub>2</sub> sintered specimens' show uniformly sized grains of average size less than 10µm.

Liquid phase sintering can produce smaller grains than that formed by solid state process. it can be concluded that the

effect of NiO addition was demonstrated not only by the decrease of the sintering temperature, but also by densification of ZnO-NiO-SiO<sub>2</sub> ceramics. SEM of mix S<sub>2</sub> is shown in Fig. 5. There are different shades, the main bulk formed of grains of ZnO with smaller white nodal shaped grains, lying intergranularly. EDAX of these grains indicate that they are a mixture of Ni and Zn. The decrease of grain

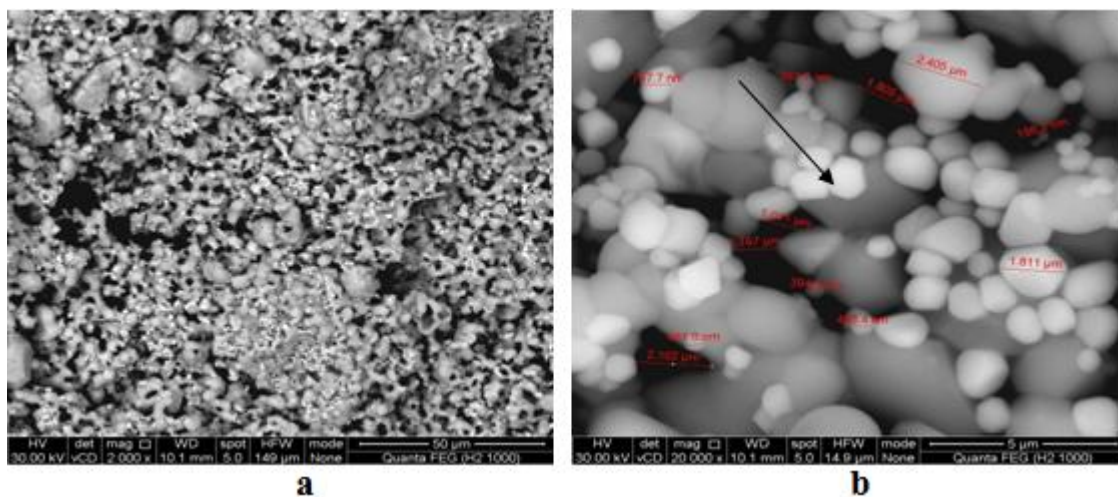
size is attributed to the precipitation of secondary phase in the grain boundaries and nodal points. The presence of 0.1 wt% ZrO<sub>2</sub> remained as chemically stable second phase particles among ZnO grains, and thus retarded densification and inhibited the grain growth of ZnO in the liquid phase sintering.



**Figure 5:** SEM of Mix S<sub>2</sub> fired at 1000 °C /2h . (a)Thermally etched ,general view. X=2000 (b)Thermally etched shows euhedral grains of ZnO randomly oriented. X=20000 (c) EDAX of nodal shape in sample S<sub>2</sub>

Fig. 6. shows the microstructure of the as-prepared ZnO-NiO-SiO<sub>2</sub> micro composite (mix S<sub>3</sub>) . The ZnO grains are homogeneous, NiO SiO<sub>2</sub> particles are small and distributed at the boundary of the ZnO grains. Elementary composition analysis by EDAX confirms that the Ni and Si contents are

higher near the grain boundary than in the matrix (ZnO), indicating the formation of a Ni - rich phase along the ZnO grain boundaries.



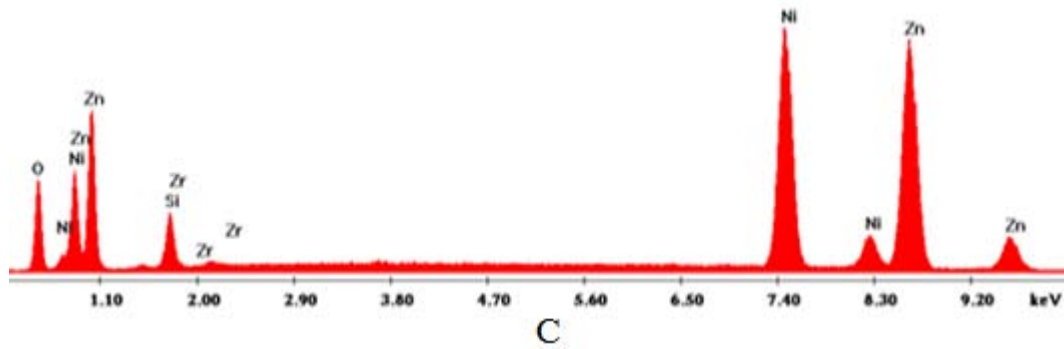


**Figure 6:** SEM of Mix S3 fired at 1000 °C / 2h  
 (a) Thermally etched, general view. X=2000

(b) Thermally etched shows oval shape of Ni- rich phase between grains of ZnO. X=20000 (c) EDAX of oval shape in sample S<sub>3</sub>

Fig. 7. SEM of sample S<sub>5</sub>, shows the segregation of the intergranular phase in patches. This is evident from the different shades displayed varying from dark grey – light grey and white. The samples were of very dense microstructure. Although some pores were present, they

were very small and separated from one another. The decrease of grain size is attributed to the precipitation of secondary phase in the grain boundaries and nodal points.

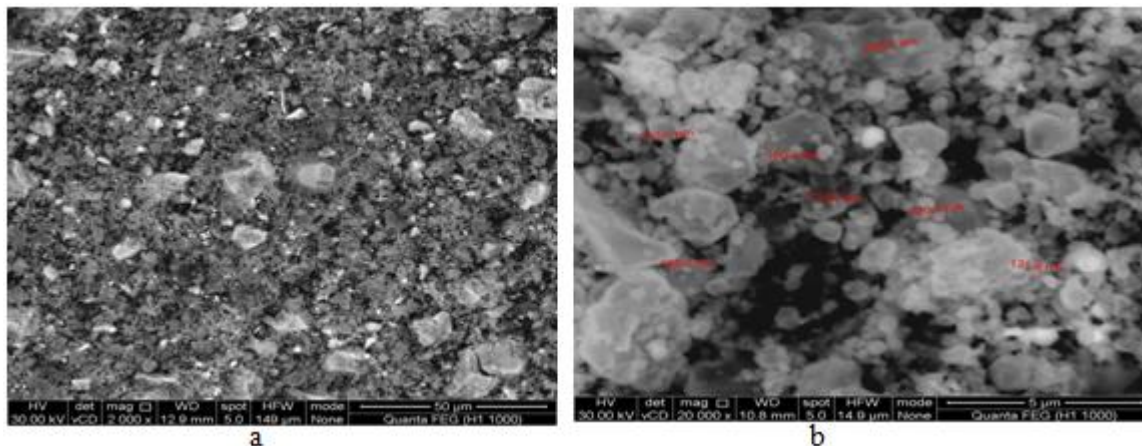


**Figure 7:** SEM of Mix S5 fired at 1000 °C / 2h .  
 (a)Thermally etched ,general view. X=2000

(b) Thermally etched shows intergranular phase, light in color. X=20000

Fig. 8. Shows the variation of the dielectric constant as a function of frequency for all samples. Obviously, the dielectric constant shows a decreasing trend for all the samples. The decrease is rapid at lower frequency and slower and stable at higher frequency. The decrease of dielectric constant with increasing frequency is a normal dielectric behavior which is also observed by other researchers [17-19]. A composite ceramic system is considered as heterogeneous material that can experience interfacial polarization as predicted by Maxwell and Wagner. They pointed out that at low frequency region (refer to Figure 8) the movement of charge carriers trapped at interfacial region which is caused by inhomogeneous dielectric structure. At high frequency, the dominant mechanism contributing to dielectric constant is the hopping mechanism in their respective interstice under the influence of alternating current. The frequency of hopping between ions could not follow the frequency of applied field and hence it lags behind, therefore the values of dielectric constant become reduced at higher frequency [20].

A low loss factor is desirable for a dielectric material so that the dissipated electric power to the insulator is minimized. This type of consideration is very important for high power circuits operating at high speed. Dissipation factor is a ratio of the energy dissipated to the energy stored in the dielectric material. The more energy that is dissipated into the material, the less is going to make it to the final destination. This dissipated energy typically turns into heat or is radiated as radio frequency (RF) into the air. The optimal goal is to have 100% of the signal pass through the interconnection network and not be absorbed in the dielectric. A high loss material means a little or no signal is left at the end of the transmission path. In other to retain maximum signal power, a low loss material should be used. The defect, space charge formation and lattice distortion is believed to produce an absorption current resulting in a loss factor and at high alternating frequency those could follow the field applied and later values the trend saturated [20].

As can be seen in Fig . 8 ., the  $\epsilon''$  value is reduced with increase in NiO wt. % and it start to be constant at frequency 1MHz. The reduction in the  $\epsilon''$  values is due to the structure

of the prepared sample. The low dielectric constant can be produced by having a porous structure. The graphs of dielectric constant with frequency are shown in Fig. 6. From these figures, it can be seen that the dielectric constant initially decreases rapidly with increase in applied frequency up to a certain frequency 1 kHz and beyond that remains fairly constant for all the compositions. The decrease in dielectric with increase in applied frequency is also reported for Cu-Zn ferrites [21-22]. This behavior may be due to the existence of interfacial polarization [23]. Dielectric properties are mainly governed by the conduction mechanism in ZnO-NiO-SiO<sub>2</sub> micro and nanocomposite, where in electron hopping takes place. This electron hopping looks to be favorable at lower applied electric field frequencies. Therefore, at lower frequency the dielectric constant is maximum. The dielectric behavior for the present samples can be explained on the basis that the mechanism of polarization process in ferrites is similar to that of conduction process.

In normal dielectric behavior, the dielectric constant decreases with the increasing frequency reaching a constant value. Dielectric thicknesses are the important parameters that will influence capacitor performance. Since the

capacitance is porosity dependence and from the formula, capacitance is directly proportional to the dielectric constant of the material, hence the reduction in the dielectric constant value also due to the porosity produced in the specimens as shown in Figs (5-8). It is seen that the dielectric constant of the composites gradually decreases with increase in SiO<sub>2</sub> filler content. It is a well-known fact that the dielectric constant of SiO<sub>2</sub> filler is 3.8. Thus; the resultant dielectric constant of combined ZnO-NiO-SiO<sub>2</sub> micro composite gradually decreases with increasing SiO<sub>2</sub>. The highest value of permittivity at 1 kHz at room temperature, and an evident dependence of frequency is recorded for 30% NiO addition to ZnO+SiO<sub>2</sub> composite ceramics sintered at 1000°C which is characterized by a uniform microstructure and highest density i.e. The variation in dielectric permittivity behavior hardly can be related only to the differences in microstructure, since the grain sizes are similar in most of the specimens. The relation between resistivity and frequency for different mixes are shown Fig. 9. This figure shows that the AC resistivity decreases with increasing frequency at room temperature. This may be attributed to the increase in the number of dipoles and consequently increases the hopping probability. Also the increase of frequency decreased the resistivity because it increases the ionic response to the field variation.

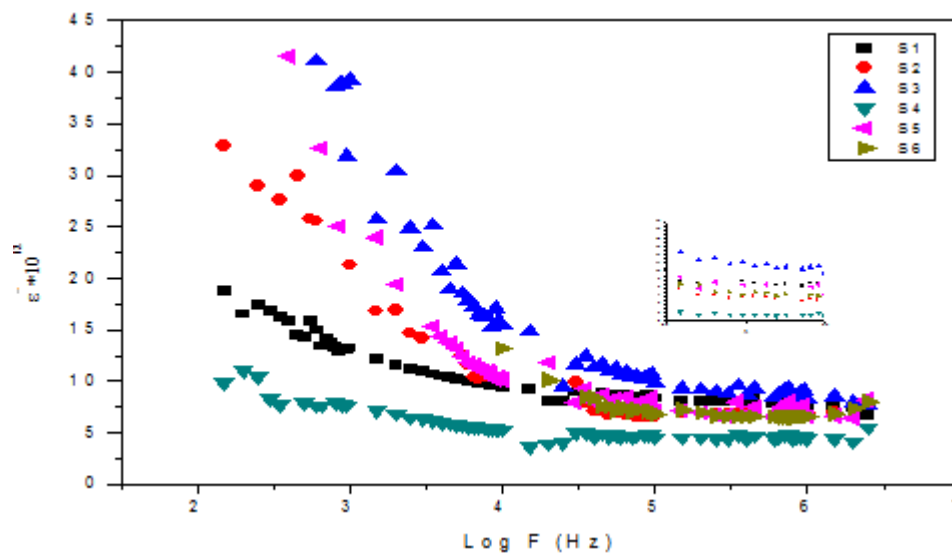


**Figure 8:** The frequency dependence of the dielectric constant

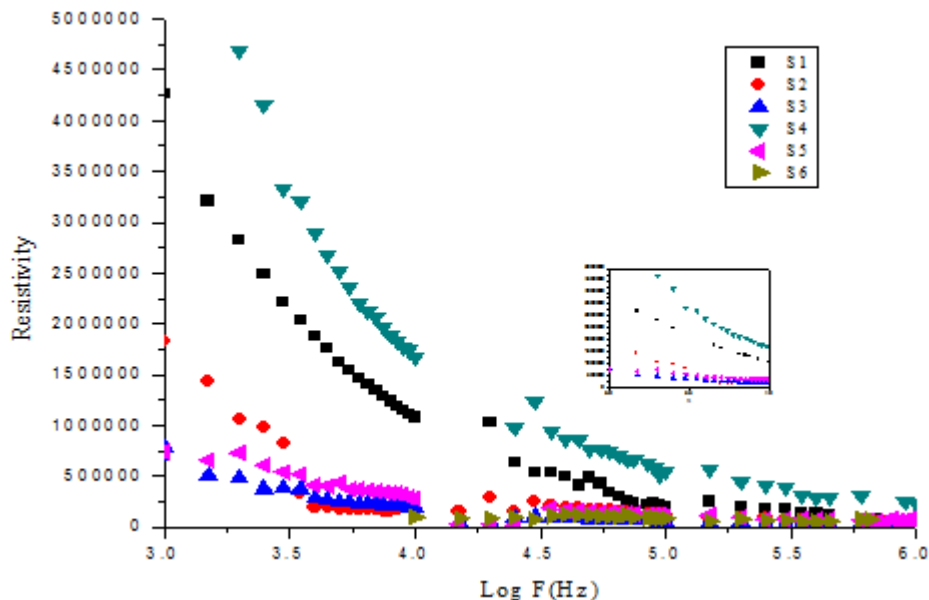


Figure 9: AC resistivity as a function of frequency at room temperature of different mixes

#### 4. Conclusions

- 1) Addition of SiO<sub>2</sub> in the presence of ZnO and NiO leads to better densification by minimizing the present of closed pores. Results of firing shrinkage as a function of temperature show increase of shrinkage with temperature.
- 2) The relative density for the samples increased as the NiO content increased; also it decreased as the SiO<sub>2</sub> content increased.
- 3) The dielectric constant shows a decreasing trend for all the samples, the decrease is rapid at lower frequency and slower and stable at higher frequency.
- 4) The AC resistivity decreases with increasing frequency at room temperature. This may be attributed to the increase in the number of dipoles and consequently increases the hopping probability.

#### References

- [1] M.Peko Jean-Claude, L .Deusdedit. JR .Spavieri., L. Charles. Da Silva, Carlos A. Fortulan, Dulcina P.F. de Souza, Milton F. De Souza, Solid State Ionics, 156 (2003) 59.
- [2] Y.Sahin, Kompozit Malzemelere Giriş, Gazi Üniversitesi, (2000).
- [3] K.M. Shu, G. C. Tu,. Materials Science and Engineering (2002) 236.
- [4] C. Aksu Canbay Master Thesis, Firat University , Graduate School of Natural and Applied Sciences, Elazığ-TURKEY, (2005).
- [5] J.Lu, Z.Ye, L. Wang, J. Huang, B.Zhao, Materials Science in Semiconductor Processing, 5, (2003) 491.
- [6] Y. Natsume, Sakata, H. *Materials Chemistry and Physics*, 9594 (2002) 1.
- [7] S.V. Han, D.H. Lee, V.J. Chang, S.O. Ryu, T.J. Lee, C.H. Chang. *Journal of the Electrochemical Society*, 153(6), (2006) 382.
- [8] V.R. Shinde, C.D. Lokhande, R.S. Mane, H. Sung-Hwan, *Applied Surface Science*, 245, (2005) 407
- [9] B.N. Wang, O.Y. Li, Z.R. Nie, Z.H. Wang, Q. Wei, *Journal of Colloid and Interface Science*, 320, (2005) 254.
- [10] Q.Li, S.J. Wang, P.C. Lim, J.W. Chai, A.C.H. Huan, C.K. *Thin Solid Films* 462 (2004) 106.
- [11] W. Bekhti, M. Ghamnia, *Catalysis Today*, 89, (2004) 303.
- [12] N. Rana, P. Raghu, E. Shero, F.Shadman, *Applied Surface Science*, 205 (2003)160.
- [13] A.C. Canan, A. Ayse, *Turkish Journal of Science and Technology*, 4(2), (2009)121.
- [14] V. Mohammad, *Theories and Applications of Chemical Eng.*, 14(2) (2008)
- [15] M.A. Vidales-Hurtado, A. Mendoza-Galvan, *Materials Chemical and Physics*, 107(2008) 33.
- [16] G.H. Chen, X.Y. Liu, *J. Mater. Sci.: Mater. Electron.* 15 (9) (2004) 595.
- [17] H. Chenari. Mahmoudi, Ali Hassanzadeh,\*, M.M. Golzan, H. Sedghi, M. Talebian ,*Current Applied Physics* 11 (2011) 409.
- [18] B. H. Venkataraman, K.B.R. Varma, *Solid State Ionics* 167 (2004) 197
- [19] D. Ravinder, G. Ranga Mohan, Prankishan, Nitendarkishan, D.R. Sagar, *Materials Letters* 44 (2000) 256.
- [20] Kumar, G. B. and Buddhudu, S. *Ceram. Int.* 36, (2010)1857.
- [21] S.G. Kulkarni, Ph.D. Thesis, Shivaji University, Kolhapur, 1995. [21] A.Y. Lipare, Ph.D. Thesis, Shivaji University, Kolhapur, 2002.
- [22] A.Y. Lipare, P.N. Vasambekar, A.S. Vaingankar, *Mater. Chem. Phys.* 81 (2003) 108.
- [23] M.A. Abdullah, A.N. Yusoff, *J. Alloys Compounds* 233 (1996) 129.